Cooperative Search and Survey using Autonomous Underwater Vehicles (AUVs)

Seokhoon Yoon and Chunming Qiao
Department of Computer Science and Engineering
State University of New York at Buffalo
Email: {syoon4,qiao}@cse.buffalo.edu

***Abstract*—In this work, we study algorithms for cooperative search and survey using a fleet of AUVs (Autonomous Underwater Vehicles). Due to the limited energy, communication range/bandwidth, and sensing range of the AUVs, underwater search and survey with multiple AUVs brings about several new challenges when a huge amount of data needs to be collected, and any AUV may fail unexpectedly.**

To address the challenges and meet our objectives of minimizing the total travel time and distance of AUVs, we first study a simple strategy called *Lane Based Search (LBS)*. Then, we propose a cooperative rendezvous scheme, *X Synchronization (XS)*, which enables AUVs to coordinate their data aggregation, control signal dissemination, and AUV failure detection/recovery operations via mobility-assisted data communication. We also devise a way to calculate appropriate timeout periods used to detect an AUV failure and describe how surviving AUVs subsequently carry out the survey mission. Numerical analysis and simulations have been performed to compare the performance of XS and other rendezvous schemes. The results show that XS can outperform other rendezvous schemes in terms of the total survey time and the travel distance of AUVs.

I. Introduction

Recent development in technology of acoustic and magnetic sensors, underwater communication devices, and especially autonomous underwater vehicles has enabled comprehensive underwater monitoring for various applications. In this paper, we propose an architecture for cooperative search and survey using a fleet of AUVs. This work targets the time-sensitive search and surveying applications (e.g. underwater surveillance, search/rescue operation, or seismic monitoring) in a large area without using any pre-existing infrastructure such as observatory/cabling, while at the same time, requiring the ability to deal with possible AUV failures.

A. Design Consideration

Given the targeted applications, our major design considerations include

- Load Balancing and Energy Efficiency: Since AUVs have limited energy source, the amount of search and survey load (in terms of area or distance covered) should be evenly distributed among AUVs.

Also, the total search and survey distance and time should be minimized to achieve overall efficiency.

- Directional Search: In a search or rescue operation, directional search is desirable especially in the presence of a strong underwater current. The fleet of AUVs should begin a survey from a position, where a target (e.g. a wrecked ship/airplane) is likely located, to the direction in which the target is likely to move. Further, even for a normal survey, surveying in the same direction of the underwater current will be more energy efficient.
- Fault Tolerance: The fleet of AUVs are required to complete the survey in the presence of AUV failures due to a mechanical and/or communication problem. Therefore, AUVs should perform the failure detection/recovery as soon as possible to minimize the survey completion time.
- Data Aggregation and Control Signal Disseminiation: For timely reaction to intermediate findings during search and survey, data collected by AUVs need to be aggregated and sent to either one or more specially equipped AUVs or a mothership (or basestation) for analysis. The need for data aggregation may also arise due to the fact that the AUVs may have a limited storage capacity on board due to size, weight, and power consideration, especially if high resolution data (e.g. high quality video or photo image) is to be collected over a large area. In such a case, data aggregation can alleviate the problem since data can be consumed (or at least compressed) by a sink node (e.g. a powerful AUV or mothership). Conversely, during the search and survey process, control signals (including requests and commands) from the mothership or an AUV may need to be disseminated to other AUVs to respond to certain events (which may or may not be triggered by the intermediate findings).

As to be discussed in Section II, existing approaches relying on a single AUV or infrastructure (e.g. cabling and fixed observatories) for underwater monitoring are no longer effective for the targeted applications. In addition, no existing works using cooperative mobile nodes take the above design considerations into account.

B. Overview

Based on the design considerations discussed above, instead of requiring the fleet of AUVs to be connected to each other and in particular be in a certain formation as in previous works on cooperative mobile nodes, we consider a simple survey strategy, Lane Based Search (LBS). In LBS, the survey area is partitioned into several sub-areas, each being assigned to one AUV, which collects data of interest (e.g. bathymetric mapping data or photo/video image) in the sub-area in the appropriate direction. Note that, given a large area and a small number of AUVs, the width of each sub-area may exceed the communications (and sensing) range of each AUVs. Accordingly, this differentiates our work from those requiring the fleet of AUVs to be connected to each other and in particular be in a certain formation as in previous works on cooperative mobile nodes.

Each AUV is assumed to be able to calculate its

location using onboard sensors (e.g. Doppler Velocity Log, a gyrocompass, and a pressure sensor) based on its previously known location (e.g., the point of the initial deployment). To minimize the positioning error, each AUV periodically updates its location via an acoustic signal from a mothership [1] or other AUVs that have recently updated their locations. We also consider the possibility that one or more AUVs may have more powerful computing resources for data analysis, or can communicate with the mothership via a long range acoustic channel (or an optical cable) to send collected data and receive control signals. Such a powerful AUV will become the *Lead* AUV and the rest become *Member* AUVs of the fleet. This is illustrated in Fig. 1. Note that our scheme, to be described in more detail below, will still be useful even if all AUVs are equal and there is no mothership since coordination among AUVs via control signal dissemination for AUV failure resilience for example is still needed.

More specifically, for failure detection/recovery of AUVs, data aggregation, and other coordinated operations, AUVs need to communicate with each other. However, the width of each sub-area can be wider than the data communication range of each AUVs due to limitations of underwater communication [2]–[4]. Even the two AUVs assigned to the neighboring sub-areas may not be able to transfer data with each other at all times, except when they move close to each other towards the common border. For instance, to achieve 500 kbps data rate, the distance between two communicating peers should be less than or around 60 meters in a deep water by using PSK modulation technique [3]. Alternative communication technologies also require short transmission range for a higher data rate (e.g. 10 Mbps data rate can be achieved with a transmission range about 20 meters using underwater optical link [5]). Accordingly, the AUVs form a intermittently connected network (ICN) or disruption/delay tolerant network (DTN) in which the AUVs are not always connected to one another. Therefore, the main challenges are to enable AUVs to perform mass data communication (or control signal dissemination) without significantly increasing energy consumption and survey completion time in the ICN/DTN environment, and to survive possible AUV failures.

To address the above challenges, we propose a cooperative rendezvous schemes, *X Synchronization (XS)*, in which AUVs periodically meet for synchronization while surveying an area. During synchronization, data and control signals including updated positioning information are relayed among AUVs via mobility-assisted communication in a multi-hop fashion. XS enables AUVs to perform synchronization without any extra movement, as AUVs determine the RP (Rendezvous Point) where synchronization occurs along the survey path. In addition, XS allows AUVs to determine the frequency of synchronization such that the survey completion time is minimized. XS also provides resilience to AUV failures by detecting the failure and then covering the sub-area allocated to the failed AUV with the surviving AUVs.

As shown in Fig. 1, each AUV performs the survey and, when an AUV moves close to its neighbor, it forwards sensor data or control signal to the neighbor.

For example, the sensor data that A_5 has collected is forwarded to A_4 at T_1. Then, at T_2, the data is again forwarded to A_3 (Lead AUV) where sensor data is aggregated. In a similar way, the control signals are disseminated from the Lead AUV to the member AUVs.

In this work, we also determine appropriate synchronization timeout values to be used in XS to reduce the number of false alarms while being able to detect actual failures as soon as possible. A numerical model is also devised to approximate the survey time and traveling distance, and verified through simulations. Both numerical analysis and simulation results show that XS outperforms two other rendezvous algorithms, Alternating Columns Synchronization (ACS) and Strict Line Synchronization (SLS) which we have also considered.

The rest of the paper is organized as follows. Section II discusses related works. In Section III, a basic survey architecture including LBS is described. Section IV introduces other rendezvous schemes and presents the proposed XS. Section V derives an appropriate timeout period for failure detection. Sections VI and VII evaluate the performance of XS through numerical analysis and simulations respectively. Section VIII concludes the paper.

II. Related Works

A. Oceanographic Monitoring

Recently, many underwater observation projects have been carried out using new technologies (e.g. sensors, acoustic communication, and AUVs), which have enabled scientists to pursue new approaches to the oceanography studies.

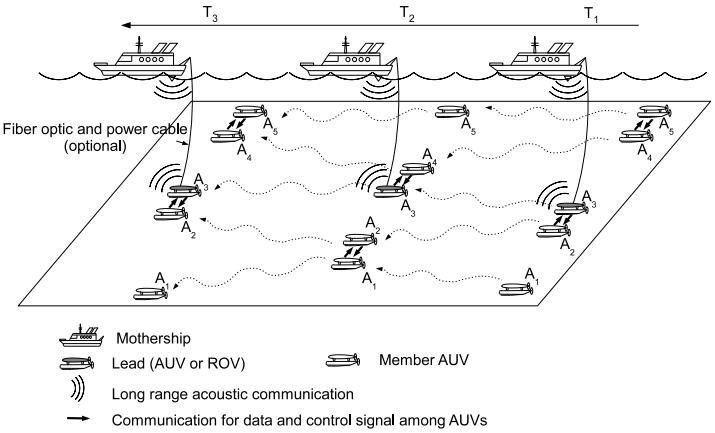

Fig. 1. Underwater survey with cooperative AUVs

The projects in [6], [7] established a long term underwater observatory. In particular, the Neptune project [6] established a plate-scale fiber-optic/power cable connected undersea observatory network on the Juan de Fuca tectonic plate. The electro/optical cable provides high power and communication bandwidth to the observatories for real-time and long-term four dimensional remote oceanographic studies (e.g. ocean dynamics, marine organisms, plate tectonics, and biogeochemical cycles). Thirty Neptune nodes are spaced approximately 100 km apart which leads to thousands of kilometers of cable length in a mesh topology. The network of those nodes serves as a fixed infrastructure for the oceanography studies. In contrast, our work focuses on the flexible, short-term, and on-demand oceanographic monitoring problem in areas without infrastructure.

The works in [8], [9] used a single AUV for the oceanographic study. In [8], an AUV is deployed for 45 hours to survey a $48km^2$ coral mound field in the Straits of Florida, while in [9] an AUV, which carries

various sonar magnetic and camera based sensors, had to make 165 dives to survey a distance of about 2500 km for the seafloor dynamics study [10], [11]. Accordingly, they are applicable to a relatively small area or relatively long-term project. Meanwhile, our work focuses on the time-sensitive search and survey applications in a large area using multiple cooperative AUVs.

In [12], authors reported the experimental results from using three AUVs in Monterey Bay based on adaptable formation control of constantly-connected AUVs (instead of intermittently connected AUVs studied in our work). It also differs from ours in that their works focus on the gradient climbing and feature tracking problem instead of minimization of the survey time and traveling distance.

B. Underwater Communication and Networking

There have been a lot of works on underwater communication and networking [2]–[5], [13]–[15]. [2]–[4] studied issues of designing reliable underwater acoustic networks. In particular, the work in [2] discussed the challenges of underwater networking due to power limitation and the underwater acoustic communication characteristics such as limited bandwidth, high level of multi-path effect and fading, high propagation delay and bit error. The study in [3] summarized the development of modulation techniques and corresponding achievable data rates and transmission ranges. [3] also discussed disadvantages of acoustic channel for a long distance communication, and proposed to use short-range underwater acoustics based multi-hop acoustic network. In [4], it was shown that multi-hop underwater communication can be more energy efficient than a long single hop communication.

Alternative underwater communication technologies have also been studied for short-range high data rate communication [5], [16], [17]. [5] showed that up to 10 Mbps data rate can be achieved for the range of 20m using directed light transmitters. [16] studied preliminary design of optical communication system using omnidirectional optical transceiver to achieve up to 10Mbps data rate. [17] studied underwater communication based on electric current for low power and short distance communication, and showed that it can potentially achieve about 1 Mbps data rate. These and other related studies show that our assumptions on limited sensing and (high data rate) communications ranges are reasonable.

C. Cooperative Operation of Mobile Nodes

There also have been studies on applications of mobile sensor nodes. The works in [18] [19] studied movement assisted sensor deployment, [20] showed mobile sensor nodes increases the sensing coverage, and [21] studied a triangulation-based sensor coverage algorithm using three mobile sensor nodes. Individual mobile sensor node technologies such as AUVs [22], UAVs (Unmanned Aerial Vehicle) [23], and autonomous vehicles [24] also have been studied.

The works in [25]–[27] studied natural phenomenon of cooperative flocking or swarming. [28], [29] proposed algorithms for cooperation of mobile nodes inspired by those biological behaviors. [30] proposed a team

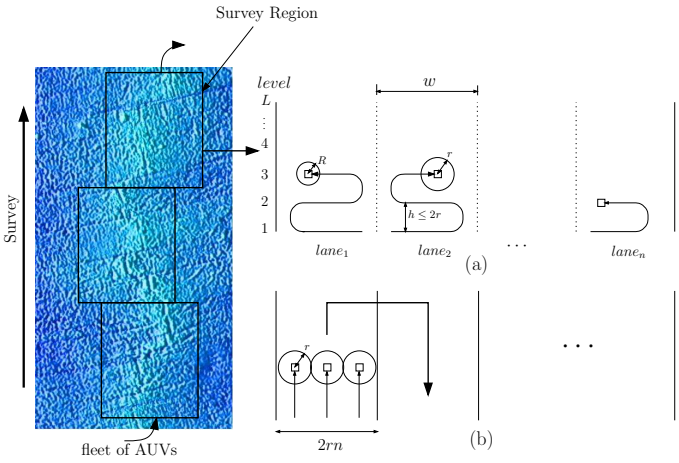

Fig. 2. Oceanographic Survey Strategy: Lane Based Search

architecture of robotic agents for surveillance in a small area (office or lab environment) where ranger nodes carry and deploy a set of scout nodes that have a video camera and motion detector.

However, these works assume that mobile nodes form a constantly connected network, while in our work AUVs form a delay tolerant network. In addition, none of these works addressed the survey problem in a large area using a potentially large number of cooperative mobile nodes.

III. Underwater Survey: Basic Architecture

In this section, we discuss the basic underwater survey architecture. We first describe the Lane Based Search strategy where each AUV is assigned to an equal sized sub-area. Then, we introduce synchronization among AUVs which enables AUVs to employ mobility-assisted communication for coordinated operations including sensor data aggregation, control signal dissemination, and detection/recovery of AUV failures.

A. Lane Based Search

Fig. 2 shows an example of oceanographic survey along the mid-ocean ridge [31] to obtain ocean bathymetric data (e.g. volcanic tectonic features, ocean morphology, or hydrothermal vents). In our survey architecture, one or more survey regions are first determined as shown in Fig. 2. The properties of each survey region (such as location, size, and shape) depend on many factors including the purpose of the survey, the number of AUVs, and battery life of each AUV. Determination of survey regions are beyond the scope of this work, and we assume that survey regions are given.

Lane Based Search (or LBS) strategy is used to cover each survey region as shown in Fig. 2 (a). A survey region of H x W units is partitioned into n sub areas of equal size, where n is the number of AUVs. Each sub area, called a lane hereafter, is H x w units where $w = \frac{W}{n}$ (the width of a lane). Each AUV is assigned to one lane, and an AUV is responsible for surveying its designated lane. Let r be the sensing range of each AUV. If the width of lane, w, is less than $2r$ (the survey swath of each AUV), AUVs move only forward in the survey direction. In practice, in a large survey area, however, w can be much larger than $2r$. In that case, an AUV has to move horizontally as well as forward (following a snake like path) as illustrated in Fig. 2. The survey area can thus be considered to have multiple levels lengthwise, and the height of each level, h, has to be less than or equal to $2r$ to avoid any sensing coverage hole. In addition, since the width of a lane can also be wider than the data transmission range, R, an AUV has to move

close to the borders of its lane in order to communicate with its neighboring AUVs for relaying data.

An alternative survey strategy is that the AUVs move in a formation (e.g., a simple line) to sweep the area either vertically or horizontally. In other words, as shown Fig. 2 (b), the entire formation moves in the same snake-like fashion (in sync with each other) as each individual AUV does in LBS except that the width of the "lane" assigned to each AUV in this alternative approach is much narrower than in our approach. Note that, in practice, it is very difficult to maintain a formation as it requires each AUV to make constant adjustments to keep in sync with each other. In addition, this alternative approach may not be effective for the problem under consideration. For example, when the (data) communication range of an AUV is smaller than the swath width as determined by the sensing range r of the AUV (i.e. $R < 2r$), keeping the AUVs close to each other in order to maintain the formation will result in overlapped sensing areas which may be unnecessary and thus resulting in an overhead.

In addition, the alternative strategy may require more energy consumption especially for a large survey area. To compare the energy consumption of the LBS and the alternative strategy, we derive a simple energy consumption model based on the traveling distance of the AUVs. For simplicity, suppose a square survey region of W x W units and all AUVs are initially deployed at their starting point by mothership. Also let $d = 2r$.

In LBS, the region is partitioned into n lanes, each of which has a width of $\frac{W}{n}$. For the survey, an AUV first moves the distance of $\frac{W}{n} - d$ for the horizontal survey at each level (note that an AUV does not need to move up to the border line of lanes due to the sensing range r). Then, it moves vertically to the next level. The total number of levels is $\frac{W}{d}$, and the total travel distance for the vertical movements is $W - d$ for each AUV. Therefore, the total traveling distance of all AUVs, S_{lbs}, becomes

$$S_{lbs} = n\left(\frac{W}{d}\left(\frac{W}{n} - d\right) + W - d\right) \quad (1)$$

$$= \frac{W^2}{d} - nd \quad (2)$$

When the alternative approach is used, the fleet of AUVs have the vertical survey as many as $\lceil \frac{W}{dn} \rceil$ times, which results in the total distance of $(W - d) \times \lceil \frac{W}{dn} \rceil$ for the vertical survey of each AUV. After a vertical survey, each AUV moves horizontally by the distance of dn. During survey, each AUV has the horizontal movements as many as $\lceil \frac{W}{dn} - 1 \rceil$ times. For simplicity, let $\frac{W}{dn}$ be an integer number. Then, the total traveling distance of AUVs becomes

$$S_{alt} = n\left[(W - d) \times \frac{W}{dn} + dn\left(\frac{W}{dn} - 1\right)\right] \quad (3)$$

$$= \frac{W^2}{d} + (n-1)W - dn^2 \quad (4)$$

Suppose that both LBS and the alternative approach consume the same amount of energy for traveling a unit distance. Then, to compare the energy consumption between two approaches, we show $S_{alt} - S_{lbs} > 0$.

Note that $\frac{W}{dn} \geq 2$ i.e. $W \geq 2dn$ (if $\frac{W}{dn} = 1$, the LBS and the alternative approach will have the same survey path, which will result in the same traveling distance).

Then, from (2) and (4), $S_{alt} - S_{lbs}$ becomes

$$\begin{aligned} S_{alt} - S_{lbs} &= nW - W - dn^2 + dn & (5) \\ &\geq 2dn^2 - 2dn - dn^2 + dn & (6) \\ &= dn(n-1) & (7) \end{aligned}$$

For $n > 1, d > 0$, (7) is greater than 0. Therefore, AUVs in LBS travel less distance than those in the alternative formation based approach.

B. Periodical Synchronization among AUVs

Due to the differences in the speed of the AUVs and the limited range of mass data communication, synchronization among AUVs is required in order for AUVs to relay data, detect an AUV failure, and cooperate with other AUVs. In our scheme, synchronization between neighboring AUVs occurs at select RPs (Rendezvous Points), which are agreed upon locations predetermined by the synchronization scheme.

The following processes are performed during a synchronization among the AUVs.

- Data aggregation: The collected sensor data of AUVs are aggregated at the Lead AUV.
- Control signal dissemination: Control signals (from the Lead AUV or the mothership) are forwarded to all AUVs.
- AUV failure detection: AUVs use a timer to detect possible AUV failures and cooperate with other AUVs to confirm the failure.
- Failure recovery: One AUV is chosen as a recovery node, and goes back up to the last RP to cover the failed AUV's area. Further, the lanes are changed in size and number according to the remaining AUVs, and reassigned to the AUVs.
- Rejoining of a recovery node: After the recovery of a failed AUV, the recovery node catches up with other AUVs and rejoins the fleet.

IV. X Synchronization (XS)

In this section, we first introduce two basic synchronization schemes, Alternating Column Synchronization (ACS) and Strict Line Synchronization (SLS), then propose X Synchronization.

A. Alternating Column Synchronization (ACS)

In ACS, every AUV (except for A_1 and A_n) meets a sync peer (one of its neighboring AUVs) at every other level as shown in Fig. 3. If an AUV (e.g. A_{i-1}) meets one of its neighbor (e.g. A_{i-2}) at $level\ j$, it meets its *other* neighbor (e.g. A_i) at $level\ j+1$. The AUV, which arrives at an RP earlier than its sync peer, waits for the sync peer until it arrives at the RP or a timeout occurs. If the sync peer reaches the RP before a timeout, they perform synchronization. During synchronization, the AUV further from the Lead AUV forwards data (that it has generated and received from its other sync peer) to the AUV closer to the Lead AUV, while the control signals are also forwarded in the opposite direction.

On the other hand, if an AUV (e.g. A_{i-2}) has a timeout, it moves toward the failed AUV's (e.g. A_{i-1}) other sync peer (e.g. A_i) in order to confirm the failure. As long as there is at most one AUV failure at a time, the two neighboring AUVs of the failed AUV will eventually see each other to confirm the failure of their common

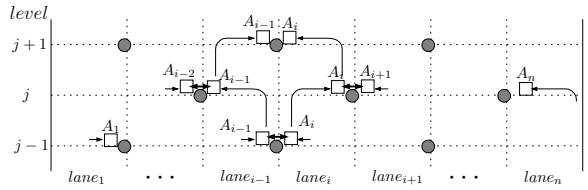

Fig. 3. Alternating Column Synchronization

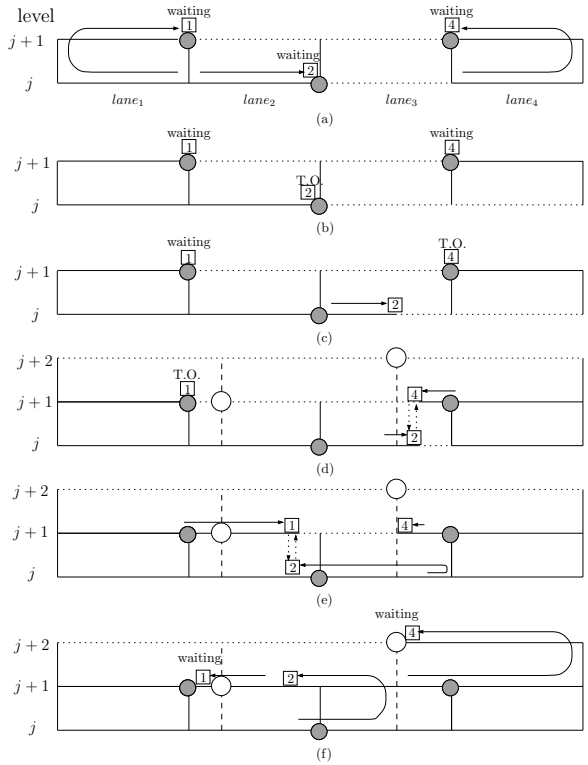

Fig. 4. Failure Detection and Recovery in ACS

neighbor. Note that to use ACS it is assumed that $R \geq h$ and there is only one AUV failure at a time (XS and SLS do not have these constraints). After the failure confirmation, the AUV at a lower level (e.g. A_{i-2}) goes back at most one level to cover the failed AUV's area. Afterwards, the AUV rejoins the other surviving AUVs, and the fleet of AUVs continue the survey.

1) AUV Failure Detection and Recovery in ACS: When A_k $(1 < k < n)$ fails at an arbitrary $level\ j$, both of its neighbors A_{k-1} and A_{k+1} (or sync peers) will have a timeout at different moments at either $level\ j$ and $level\ j+1$ or $level\ j+1$ and $level\ j$ respectively. As an example in Fig. 4(a), A_3 has failed, and A_2 and A_4 have a timeout event in Fig. 4(b) and Fig. 4(c) respectively. Immediately after having a timeout, neighboring nodes of the failed AUV move to meet each other along the cross line over the lane of the failed AUV up to a distance of $2w$. The maximum level difference between the neighbors of the failed AUV is only 1, and hence the AUV with an earlier timeout definitely meets the other sync peer of the failed AUV within a distance of $2w$. If either one of those AUVs sees A_k while moving to each other, the timeout event is false (they may have had an inappropriate timeout period or A_k has traveled with a much lower speed than expected). In that case, they go back to their RP and wait for A_k for a normal synchronization. If the two neighbors only see each other (e.g., A_2 and A_4 as shown in Fig. 4(d)), they confirm the failure of A_k (A_3), and re-calculate the size of lanes because there are only $n-1$ active nodes. The AUV which is at a lower level (A_2 in Fig. 4(d)) is chosen as a recovery node, and the recovery node covers the failed AUV's area at the current level. In this case, there is no need for a recovery node to move levels back, because $level\ j-1$ must have already been covered by the failed AUV. The recovery node only needs to cover $level\ j$ of the failed AUV's lane. The neighbors also forward the information about the change of lanes and the failure to other AUVs. In Fig. 4(f), there are only 3 lanes for 3 AUVs, and AUVs have new RPs represented as white circles.

Note that if A_1 (or A_n) fails, then A_2 or (A_{n-1}) will

have a timeout event, and can immediately move towards A_3 (or A_{n-2}) to inform it and the rest of the AUVs of the failure. Afterwards, A_2 (or A_{n-1}) will go one level below for recovery.

The frequent synchronization of ACS, and hence the large aggregate synchronization delay over the operation can degrade the performance in terms of the total search time. However, ACS has a quick recovery process due to the fact that a recovery node needs to go back to at most one level for covering the area of failed AUV.

B. Strict Line Synchronization (SLS)

In SLS, synchronization among AUVs occurs at RPs on designated sync lines. As shown in Fig. 5, the AUVs have a sync line after every K levels during survey. The AUVs first complete the survey in an area between two consecutive sync lines, and then perform synchronization before they continuing the survey. Every AUV (except for A_1 and A_n) has two RPs on a sync line as shown in Fig. 5. An AUV first visits the RP further from the Lead AUV in order to meet one of its sync peers. After the AUV meets one of its sync peer (which is further from the Lead AUV than the AUV itself) and receives data from that sync peer, the AUV visits its other RP closer to the Lead AUV to meet its other sync peer to forward the data. Eventually, the data is aggregated at the Lead AUV at the center of the fleet. Then, the control signal from Lead AUV is disseminated to member AUVs in the reverse order of sensor data aggregation.

If an AUV fails to reach a sync line, its two neighbors will have a timeout and meet to confirm the failure. Then,

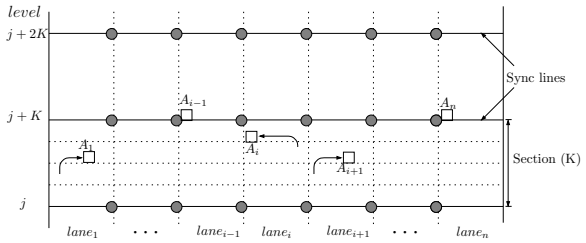

Fig. 5. Strict Line Synchronization

one of them is chosen as a recovery node, and goes back up to K levels to cover the failed AUV. Meanwhile, the remaining AUVs adjust their lane assignment to avoid any sensing coverage hole and continue the survey operation. After finishing the recovery, the recovery node will catch up with the other surviving AUV with a straight line movement and join the fleet.

1) SLS algorithm at a sync line: The fleet is divided into two groups: the left group and the right group. The left group comprises AUVs that have IDs less than or equal to $\lceil \frac{n+1}{2} - 1 \rceil$. Other AUVs belong to the right group. Here n is the number of AUVs. There are two center nodes in the middle of the fleet of AUVs, each of which belongs to a different group. As shown in Fig. 6(a), there are only $n-1$ RPs at a sync line.

Synchronization consists of two phases: the data aggregation phase, and the control signal dissemination phase. In the data aggregation phase, A_1 moves to $RP_{1,2}$ upon arrival at a sync line. For AUVs with ID greater than 1 (i.e. $i > 1$), A_i moves to $RP_{i-1,i}$ (Here we assume that A_i belongs to the left group.) If the AUV belongs to the right group, it first moves to $RP_{i,i+1}$, and has the opposite moving direction. For example, A_2 first visits $RP_{1,2}$ as shown Fig. 6(a). Note that, in Fig. 6(a), all AUVs except A_2 and A_6 have already

arrived at the sync line. If $RP_{i-1,i}$ is already occupied by A_{i-1}, then A_i receives data from A_{i-1} and moves to $RP_{i,i+1}$. In other words, A_{i-1} forces A_i to move toward the center of the fleet (e.g., A_1 and A_2 force A_2 and A_3 to move toward the center as shown Fig. 6(b) and Fig. 6(c) respectively). If $RP_{i-1,i}$ is not occupied, A_i waits for A_{i-1} until the timeout period expires or A_{i-1} arrives. In this way the two center nodes meet at an RP eventually (e.g., A_3 and A_4 in Fig. 6(g)), which means all AUVs, except for the nodes at the edges, have met both of its neighbors and relayed data. When the two center nodes meet at an RP, the Lead AUV (which is one of the center nodes) receives data of all AUVs and completes the data aggregation phase. In the control signal dissemination phase that follows the data aggregation phase, A_i receives a control signal from A_{i+1} at $RP_{i,i+1}$, and moves toward $RP_{i-1,i}$ to forward the signal. Immediately after forwarding the control signal (without waiting for the completion of the dissemination phase), A_i continues the search operation up to the next sync line.

2) AUV Failure Detection and Recovery in SLS: Suppose A_k belongs to the right group and it fails to arrive at a sync line (for example, suppose A_6 fails before it arrives at a sync line as shown Fig. 6(a)). The failure causes both of A_k's neighbors, A_{k-1} and A_{k+1}, to timeout at $RP_{k-1,k}$ and $RP_{k,k+1}$ respectively (possibly simultaneously). As an example, in Fig. 6(d), A_5 and A_7 have a timeout event at $RP_{5,6}$ and $RP_{6,7}$ respectively. Following a timeout, two neighbors move toward the lane assigned to the failed AUV. When A_k's neighbors

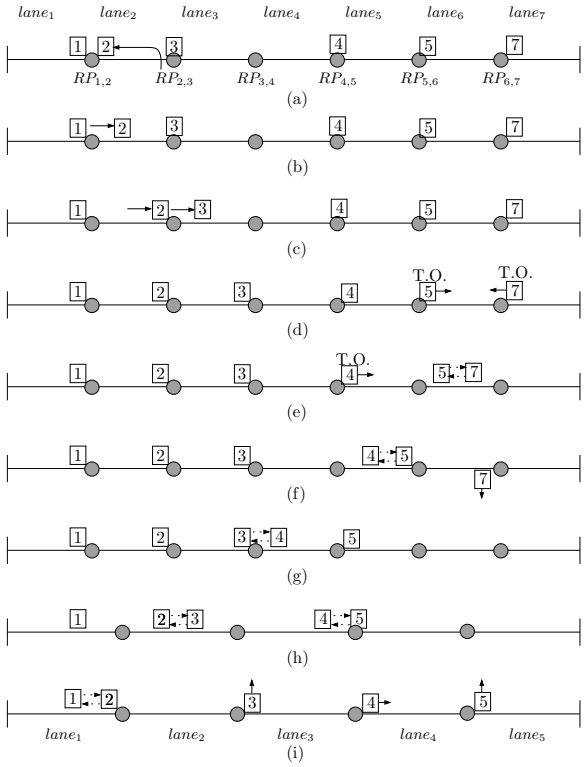

Fig. 6. Failure Detection and Recovery in SLS at a sync line

meet (A_5 and A_7 in this example), they confirm the failure, and the outer AUV among them, A_{k+1} (A_7), is chosen as a recovery node, and the inner node A_{k-1} (A_5) moves toward A_{k-2} (A_4) and informs it of the failure. As shown in Fig. 6(f), the recovery node A_7 goes back up to the last sync line to cover the area of the failed AUV. Note that other AUVs can also have a timeout event like A_4 in Fig. 6(e). The timeout causes $M4$ moves toward A_5 to see A_5 or A_6, because A_4 does not know whether A_5 has failed or A_5 has been waiting for A_6. When A_4 and A_5 meet in Fig. 6(f), A_4 learns of A_6's failure, and then it also forwards this information to A_3 in Fig. 6(g). When the Lead AUV (A_3) is informed of the failure, it performs reallocation of lanes (which results in $n-2$ lanes) and forwards this change to other member AUVs (e.g., the fleet has only 5 lanes in Fig. 6(h)). The

remaining $n-2$ AUVs in the fleet do not wait for the recovery node to return back to the sync line. Instead, they continue the search operation. After the recovery node finishes recovery, it catches up with the fleet with linear movement and rejoins the fleet by sending a rejoin request message to other AUVs. The rejoining process occurs at a sync line where the recovery node arrives earlier than other AUVs. After the recovery node rejoins the fleet, the fleet of AUVs performs reallocation of lanes and has $n-1$ lanes. Note that the recovery node knows the position of the Lead AUV, because the Lead AUV periodically broadcasts control messages containing its location with a high transmission power.

SLS may have a lower synchronization overhead than ACS because, in SLS, the fleet of AUVs does not synchronize at every level. This can reduce the total search time. However, in SLS, it may take a longer time to detect and recover from an AUV failure. Also note that, unlike ACS in which only one AUV failure can be handled at a time, SLS can handle multiple simultaneous AUV failures, because, in SLS, all surviving AUVs are on the same sync line during synchronization. In other words, after having a timeout, each surviving AUV will eventually meet its surviving neighbors on a sync line by moving until it meets another AUV or reaches the left border of the lane of A_1 or the right border of the lane of A_n.

C. X Synchronization (XS)

In XS, each AUV performs a survey in its lane individually until it reaches an area called *sync section*, where AUVs perform synchronization. After synchronization in a sync section, AUVs continue the survey individually in the following non-sync section as shown in Fig. 7.

The distance between two consecutive sync sections, K, dictates the frequency of the synchronization of AUVs. The value of K can be set to a constant value throughout the survey, or can be dynamically selected. To facilitate our presentation, we assume that K is fixed once it is chosen.

In XS, the fleet of AUVs is logically divided into two groups: the left and the right group. The AUVs whose ID is less than or equal to $\lfloor \frac{n+1}{2} \rfloor$ belong to the left group, and the rest belong to the right group. Two AUVs in the middle of the fleet are referred as center AUVs, each of which belongs to a different group. At least one of center AUVs is the Lead AUV and the other can be the backup Lead AUV.

During synchronization, data aggregation (DA) is first performed, then control signal dissemination (CSD) follows. As shown in Fig. 7, data aggregation and control signal dissemination occur along the DA segment and CSD segment.

In the following discussion, we will denote the RP at $level\ j$ for AUV i (or A_i) and AUV $i+1$ (or A_{i+1}) by $RP^j_{i,i+1}$. In XS, the RPs within each sync area form two intersecting lines that look like an "X" as shown in Fig. 7.

1) Data aggregation (DA) and Control Signal Dissemination (CSD): In this section, the algorithms of DA and CSD for the right group are described (those algorithms for the left group are similar and thus omitted). To

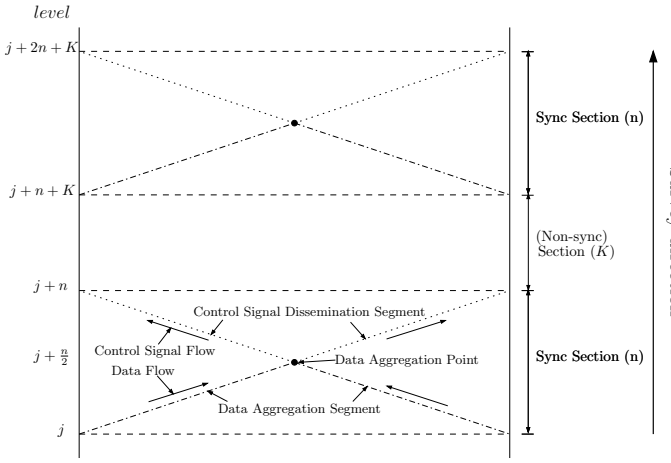

Fig. 7. X Synchronization

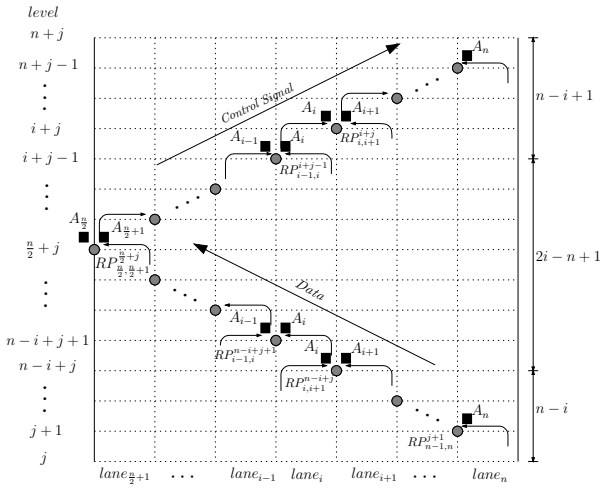

Fig. 8. XS: Synchronization of the right group

facilitate the presentations, we assume that the fleet has n AUVs where n is an even number larger than 2. Fig. 8 illustrates the synchronization process and also shows the flow of data and control signals.

Suppose that the sync section begins at $level\ j$ as shown in Fig. 8. The AUVs in the group use a slightly different algorithm depending on their relative position in the fleet as follows.

- A_i (where $\frac{n}{2}+1 < i < n$): The AUV A_i surveys its lane, $lane\ i$, until it reaches the $RP_{i,i+1}^{n-i+j}$ where A_i is supposed to synchronize with A_{i+1} at $level\ (n-i+j)$. At the RP, A_i receives the collected sensor data from A_{i+1} and appends its data to the data. Then, as shown in Fig. 8, A_i moves to its next RP at the $level\ (n-i+j+1)$, and forwards to A_{i-1} the aggregated data. Then, A_i continues the survey up to $RP_{i-1,i}^{i+j-1}$ to receive control signals from A_{i-1}. A_i also forwards the control signal to its other neighbor, A_{i+1} at the next RP at $level\ i+j$, before it continues the survey up to the next sync section.
- A_n: The rightmost AUV, A_n surveys its lane until it reaches the RP where it synchronizes with A_{n-1} at $level\ j+1$. (denoted as $RP_{n-1,n}^{j+1}$ in Fig. 8). At the RP, A_n forwards data it has collected to A_{n-1}. Then, A_n continues the survey up to its next RP at $level\ (n+j-1)$ to synchronize with A_{n-1} again and receive control signals. After receiving control signals, A_n continues the survey on its lane.
- $A_{\frac{n}{2}+1}$: A center AUV $A_{\frac{n}{2}+1}$ receives the data from $A_{\frac{n}{2}+2}$ at the RP at $level\ (\frac{n}{2}+j-1)$. Then, it moves to its next RP at the next level to synchronize with the other center AUV, $A_{\frac{n}{2}}$. If $A_{\frac{n}{2}+1}$ the Lead AUV, it receives the aggregated data of the left group, and the DA phase is completed. $A_{\frac{n}{2}+1}$ communicates with the mothership if necessary and then initiates the CSD phase to disseminate the control signal or commands.

2) AUV Failure Detection and Recovery: When A_{i-1} has a timeout while waiting for A_i at an RP, it cooperates with A_{i+1} (the other neighbor of A_i) to confirm that

A_i has really failed. The failure confirmation process is necessary, because the timeout at A_{i-1} does not necessarily indicate the failure of A_i; it is possible that A_i has been waiting for A_{i+1} at another RP. Following the failure confirmation, an AUV is chosen as a recovery node, and remaining AUVs adjust their lanes to cover the survey region without any sensing coverage hole and to re-balance the load.

Suppose A_i ($\frac{n}{2} < i < n$) fails before reaching a DA segment in a sync section which begins at $level\ j$. The failure of A_i leads to the timeouts of A_{i-1} and A_{i+1} at $RP_{i-1,i}^{n-i+j}$ and $RP_{i,i+1}^{n-i+j+1}$ respectively. After having a timeout, A_{i-1} and A_{i+1} move toward the lane of A_i as shown in Fig. 9(a). If A_{i-1} or A_{i+1} can detect the signal of A_i during their movement, the timeout is a false alarm (which is possible due to a too small timeout value). In such a case, A_{i-1} and A_{i+1} return to their RPs, and wait for A_i for normal synchronization. If A_{i-1} and A_{i+1} see each other but not A_i, as also shown in Fig. 9(a), they confirm the failure of A_i and initiate a recovery process.

Here, for convenience, we assume that R, which is a communication range of AUVs, is larger than the height of a level (e.g. $2r$). However, this constraint can be readily removed by allowing AUVs to move along the DA or CSD segment shown in Fig. 9.

After the failure confirmation, the AUV at a lower level (A_{i+1}), becomes a recovery node as shown in Fig. 9(b), and goes back to cover the lane assigned to A_i up to the previous DA segment. Meanwhile, the AUV at a higher level, A_{i-1}, moves toward its other sync peer, A_{i-2}, and informs A_{i-2}, which may or may not have a timeout event, of the failure as also shown in Fig. 9(b), and continues the survey until it reaches the CSD segment. The information about the failure is eventually delivered to the Lead AUV at $level\ (\frac{n}{2}+j)$. When receiving the failure information, the Lead AUV recalculates the width and number of lanes based on remaining AUVs and forwards a control signal containing this information of new lanes to its neighbors. A_{i-1} receives the control signal at $level\ i+j-2$ as shown in Fig. 9(c). To deal with the fact that both A_i and A_{i+1} are absent from the CSD process, A_{i-1} moves up and right towards $RP_{i,i+1}^{i+j+1}$ to forward the control signal to A_{i+2}, which may have a timeout and also been moving downward as shown in Fig. 9(d). Then, A_{i-1} moves toward its newly assigned lane, and continues the survey up to the next DA segment. After the recovery node (A_{i+1}) finishes the recovery, it will catch up with other AUVs rejoin the fleet in the first sync section encountered. Reallocation of the lanes is similar to the failure detection and recovery process.

If A_1 or A_n fails, its neighbor (A_2 or A_{n-1}) will timeout at $level\ j+1$. In this case, A_2 (or A_{n-1}) does not need failure confirmation, because it is not possible that A_1 or A_n is waiting for another AUV. Therefore, A_2 (A_{n-1}) immediately moves toward its other neighbor, A_3 (A_{n-2}) to inform it of the failure. Then, A_2 (A_{n-1}) becomes a recovery node.

If a center AUV, $A_{\frac{n}{2}}$ (or $A_{\frac{n}{2}+1}$) fails, $A_{\frac{n}{2}-1}$ and $A_{\frac{n}{2}+1}$ (or $A_{\frac{n}{2}}$ and $A_{\frac{n}{2}+2}$) have a timeout and meet to confirm the failure. After confirmation of the failure, the remaining center AUV forwards the control signal

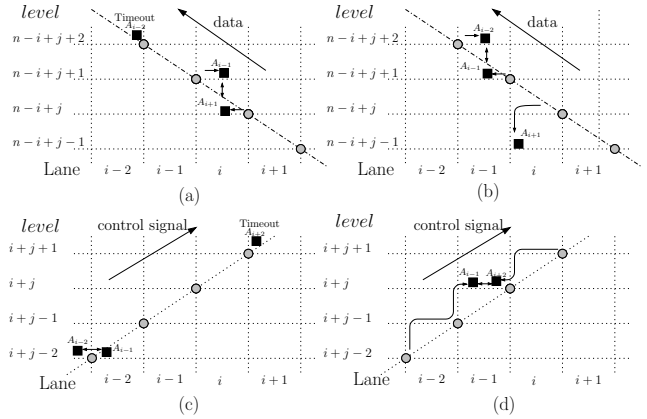

Fig. 9. AUV failure detection and recovery

to $A_{\frac{n}{2}-2}$ and $A_{\frac{n}{2}+2}$ (or $A_{\frac{n}{2}-1}$ and $A_{\frac{n}{2}+3}$).

Note that the failure of one AUV can cause successive timeouts. For example, during the DA phase, if A_i has failed, all AUVs between $A_{\frac{n}{2}+1}$ and A_{i-1} can have a timeout event while waiting for their sync peer at right. However, those cascaded timeouts will not cause any problem. More specifically, when an AUV, A_k, where $\frac{n}{2}+1 \leq k < i-1$ has a timeout, it moves toward A_{k+1} until it sees A_{k+1} and it realizes that the timeout was a false alarm and thus goes back to the normal state. Note that $A_{k'}$, where $i+2 \leq k' \leq n$, will not timeout as they have already finished the synchronization for the current DA phase.

So far, we have assumed that only one AUV failure occurs at a time. However, XS can detect and recover multiple simultaneous AUV failures. For example, in Fig. 8, if two consecutive AUVs, A_{i-1} and A_i, have failed before they reach the DA segment, A_{i-2} and A_{i+1} will have a timeout event, and they will meet eventually while moving toward the lanes of A_{i-1} and A_i respectively along RPs on the DA segment. Note that non-consecutive AUV failures can also be detected. For example, in Fig. 8, if A_{i-2} and A_i have failed, A_{i-1} and A_{i+1} will first detect and confirm the failure of A_i, and then, A_{i-3} and A_{i-1} will also detect and confirm the failure of A_{i-2} when they meet.

V. Timeout Calculation

In this section, we derive the timeout values used for failure detection in XS. A proper timeout period is required to avoid either an unnecessary wait for a failed AUV or a needless premature recovery process.

In XS, when A_{i-1} and A_i synchronize at an RP, A_{i-1} and A_i calculate the timeout value used at the next RP where they will meet again. In order to determine an appropriate timeout period for A_{i-1} and A_i, the distributions of the arrival time at the next RP of A_{i-1} and A_i are estimated. Then, A_{i-1} (A_i) chooses a timeout period such that within that amount of time, A_i (A_{i-1}) will arrive at the next RP with a high probability, say P_o, according to the estimated arrival time distribution. The arrival time distribution of an AUV at an RP is obtained using the estimated travel time distribution of the AUV from the current RP to the next RP and the delays introduced by synchronization among AUVs.

To facilitate the presentation, we first define a few variables. Let random variable $\mathbf{x_i}$ be the estimated arrival time of A_i at the next RP, and let random variable $\mathbf{t_i^y}$ be A_i's travel time for a distance of y units. Also, let $d_{p,p+1}$ ($1 \leq p < n$) represent the sync delay at an RP which is the amount of time elapsed from the arrival of the earlier AUV (between A_p or A_{p+1}) at the RP to the completion time of the synchronization between A_p and

A_{p+1}.

Suppose that AUVs, A_{i-1} and A_i, where $\lfloor \frac{n+1}{2} \rfloor + 1 < i \leq n$, synchronize with each other at an RP at $level\ u$ on a CSD segment as shown in Fig. 10. They calculate the timeout period for each other for the next RP at $level\ (u+2(n-i+1)+K)$ at the next DA segment as follows.

The arrival time of A_i is estimated first. Between the sync at $RP^u_{i-1,i}$ and the next sync at $RP^{u+2(n-i+1)+K}_{i-1,i}$, three steps should occur in the same order as shown in Fig. 10. First, the control signal is forwarded to A_n at $level\ (u+n-i)$ on the CSD segment. Then, A_n performs survey up to its next RP at $level\ (u+n-i+K+2)$. Finally, collected data are forwarded to A_i at $level\ (u+2(n-i)+K+1)$, and then, A_i moves toward to $RP^{u+2(n-i+1)+K}_{i-1,i}$ to forward data to A_{i-1}. Therefore, the arrival time of A_i is the sum of the time needed to complete these steps.

In both the CSD and DA phases, the data or control signals are forwarded through $2(n-i)$ RPs, and the distance between two RPs is $w+h$. Also suppose the synchronization at $RP^u_{i-1,i}$ occurs at time 0. Let a random variable $\mathbf{x_i}$ be the arrival time of A_i at the RP at $level\ u+2(n-i+1)+K$. Then, $\mathbf{x_i}$ can be represented as

$$\begin{aligned}
\mathbf{x_i} &= \mathbf{t_i^{(w+h)}} + \cdots + \mathbf{t_{n-1}^{(w+h)}} + \mathbf{t_{n-1}^{(w+h)}} + \cdots + \mathbf{t_i^{(w+h)}} && (8)\\
&+ \mathbf{t_n^{(w+h)(K+2)}} && (9)\\
&+ d_{i,i+1} + \cdots + d_{n-1,n} + d_{n,n-1} + \cdots + d_{i+1,i} && (10)
\end{aligned}$$

where the first line represents the sum of travel time of A_j $(i \leq j \leq n-1)$ during DA and CSD, and the second line represents the survey time of A_n for $K+2$ levels, and the third line represents the sum of sync delay among AUVs during DA and CSD.

Assume that the speeds and corresponding travel times of all AUVs have the same statistical properties i.e., $\mathbf{t_p^{(w+h)}} = \mathbf{t_{p+1}^{(w+h)}}$ (where $1 \leq p < n$). In addition, we observe that, when A_j $(i \leq j \leq n)$ arrives at $RP_{j-1,j}$ on the DA segment, most probably A_{j-1} has already arrived at the RP. This is because, for A_j to arrive at the RP, as many as $2(n-j)$ synchronization should precede at other RPs, while the arrival of A_{j-1} does not require any preceding synchronization (and A_j and A_{j-1} have an equal distance to travel). For the same reason, when $A_{j'}$ $(i \leq j' < n)$ arrives at $RP_{j',j'+1}$ on the CSD segment, most probably $A_{j'+1}$ has already arrived at the RP.

Under these observations, we assume that an AUV (the left-hand side AUV during CSD and the right-hand side AUV during DA) can begin synchronization immediately after it arrives at an RP without waiting for its sync peer. Also, for simplicity, the time to transmit data and control signals between two sync peers is assumed to be some constant value d_{sync}. From the above observations and assumptions, we have $d_{p,p+1} = d_{sync}$ where $1 \leq p < n$.

Then, (8) through (10) can be simplified into

$$\mathbf{x_i} = \mathbf{t^{(K+2n-2i+2)(w+h)}} + 2d_{sync}(n-i) \qquad (11)$$

On the other hand, $\mathbf{x_{i-1}}$, the arrival time of A_{i-1}, can be directly obtained from the travel time distribution of an AUV, because no synchronization is required for A_{i-1} to arrive at the next $RP^{u+2(n-i+1)+K}_{i-1,i}$. Therefore, $\mathbf{x_{i-1}}$

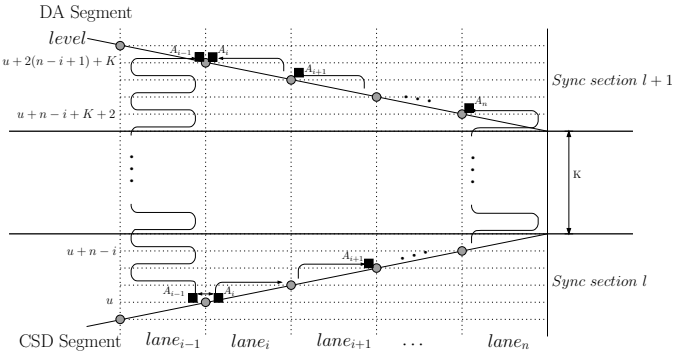

Fig. 10. Illustration for timeout period calculation for the right group

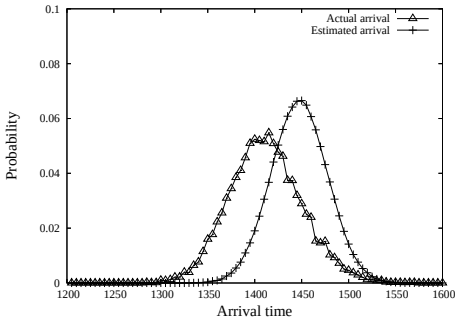

Fig. 11. Distribution of actual and estimated arrival of an AUV

becomes

$$\mathbf{x_{i-1}} = \mathbf{t}^{(\mathbf{w+h})(\mathbf{2(n-i+1)+K})} \tag{12}$$

Let $\mathbf{x}'$ be the random variable representing the arrival time of an AUV at an RP on the CSD segment. $\mathbf{x}'$ can also be obtained in a similar way that $\mathbf{x}$ is obtained, and hence, the discussion is omitted.

Now, we discuss the estimation of the travel time distribution that is used in (11) and (12). Recall that a random variable $\mathbf{t^y}$ represents the travel time of an AUV for a distance y. In order to estimate the travel time distribution of an AUV for a given distance y (e.g. between two consecutive RPs of the two AUVs), we first obtain the travel time distribution of an AUV for a distance d for some value d (which is much less than w) through simulations. More specifically, Let random variable $\mathbf{s}$ be the travel time of an AUV for a distance d, and the probability density function (pdf) of $\mathbf{s}$ be given as $f_s(s)$. Let $m = \frac{y}{d}$, then $\mathbf{t^y}$ can be represented as the sum of $\mathbf{s}$.

$$\mathbf{t^y} = \mathbf{s_1} + \mathbf{s_2} + \cdots + \mathbf{s_m} \tag{13}$$

Because $\mathbf{s_i}$ is i.i.d., the pdf of $\mathbf{t^y}$ is the convolution of $f_{s_i}(t^y)$ where $1 \leq i \leq m$. Further, according to the Central Limit Theorem, the distribution of $\mathbf{t^y}$ approaches a normal distribution if m is large enough. Specifically, let μ and σ^2 represent the mean and variance of $\mathbf{s}$ respectively, then $\mathbf{t^y}$ will approximately follow a normal distribution with the mean, $m\mu$, and the variance, $m\sigma^2$.

Let D be the total synchronization delay, then, the estimated arrival time $\mathbf{x_i}$ also follows a normal distribution with ($m\mu+D$, $m\sigma^2$) as its mean and variance. From the distribution function of $\mathbf{x_i}$, an arrival time, t_0, that corresponds to a given probability P_0 is chosen as the candidate of the timeout period (i.e. $P[\mathbf{x} \leq t_0] = P_0$).

Fig. 11 shows the probability distribution of the actual and estimated arrival time of an arbitrary AUV at its RPs during survey with a sample value of the lane width and K ($w = 550m$, K=53). The pdf of the actual arrival time was obtained through simulations. Fig. 11 shows that the actual arrival time of the AUV approximately follows a normal distribution. The timeout value, TO is chosen as $TO = \beta t_0$ where β is a design parameter to add some safety margin to reduce premature timeouts.

VI. Numerical Analysis

In this section, we discuss a mathematical models to approximate the total survey completion time and

traveling distance of AUVs using XS, which will be verified through simulations in the next section. Both AUV failure and non-failure cases will be considered.

Let *d-section* (or diamond section) be defined to be the area between two consecutive DA points (e.g. the area between $level\ k$ and $level\ k+n+K$ shown in Fig. 12).

The expected survey time for a d-section is first calculated and used in order to obtain the total survey time for the entire area. The effect of R will be also considered for more accurate approximation of the survey time.

A. The Case with No AUV Failure

1) Total Survey Time: Suppose two center AUVs meet at a DA point at $level\ k$, and complete the current DA phase as shown in Fig.12. From this moment to the completion of the next DA phase, three steps should be completed by both the left and the right groups. First, the control signal is forwarded to the A_1 (or A_n) at $level\ (k + \frac{n}{2} - 1)$. Then, A_1 (or A_n) performs the survey operation until it reaches its next RP at $level$ $(k + \frac{n}{2} + K + 1)$. Finally, data is forwarded to the center AUVs, which meet at the next DA point at $level$ $(k + n + K)$. Therefore, the survey time for a d-section will be the arrival time (at the next DA point) of the slowest center AUV between two center AUVs, after the completion of the CSD phase, the survey of K levels by A_1 (or A_n), and the DA phase.

During the CSD phase and the DA phase, the data or the control signals are forwarded through $n-2$ RPs. The distance between two RPs is $w+h$, and all AUVs, except A_1 and A_n, need to move a distance of $w + h - R$ to communicate with its sync peer. Therefore, the total travel distance of AUVs for CSD and DA is $(n-2)(w+h-R)$. Afterward, A_1 (or A_n) travels a distance of $(K+2)(w+h) - R$. Let P be the sum of the travel distance for CSD, DA, and the survey of A_1 (or A_n) in a d-section. Then, P is

$$P = (n-2)(w+h-R) + (K+2)(w+h) - R \quad (14)$$

Let random variable $\mathbf{u}$ be an AUV's travel time for the distance of P. $\mathbf{u}$ can be represented as the sum of $\mathbf{s}$ in a similar way to (13). Also let $\mathbf{v}$ be the arrival time of a center AUV at the next DA point. Then, $\mathbf{v}$ is

$$\mathbf{v} = \mathbf{u} + d_{sync} \times (n-2) \quad (15)$$

Also let $\mathbf{y}$ be the arrival time of the slowest center AUV between the two center AUVs. Then, we have,

$$\mathbf{y} = max(\mathbf{v}, \mathbf{v}) \quad (16)$$

Note that the pdf of $\mathbf{v}$, $f_v(v)$, can be obtained from the pdf of $\mathbf{u}$ and (15). From $f_v(v)$, the probability distribution function, $F_v(v)$ can also be obtained. Let $f_y(y)$ be the pdf of $\mathbf{y}$. Then, from (16), accounting for the fact that we are taking the maximum of two random variables $\mathbf{v}$'s, we have

$$f_y(y) = 2F_v(y)f_v(y) \quad (17)$$

Let $C = \frac{1}{\sqrt{2\pi m\sigma^2}}$, then the expected arrival time of

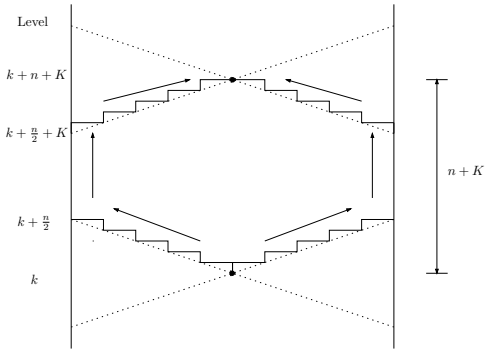

Fig. 12. Calculation of the survey time in a d-section

the slowest center AUV is

$$E[y] = \int_{-\infty}^{\infty} y f_y(y) dy \quad (18)$$

$$= 2\int_{-\infty}^{\infty} y F_v(y) f_v(y) dy \quad (19)$$

$$= 2C^2 \int_{-\infty}^{\infty} y \left(\int_{-\infty}^{y} e^{-\frac{(x-m\mu)^2}{2m\sigma^2}} dx\right) e^{-\frac{(y-m\mu)^2}{2m\sigma^2}} dy \quad (20)$$

The two center AUVs also need the time d_{sync} to exchange data. Therefore, the expected survey time for a d-section is $E[y]+d_{sync}$. The expected total survey time, T_{XS}, is the product of the survey time for a d-section and the total number of d-sections, that is,

$$T_{XS} = (E[y] + d_{sync}) \times \frac{L}{n+K} \quad (21)$$

2) Average Travel Distance of AUVs: We first calculate the total travel distance of the AUVs to obtain the average travel distance of AUVs. At every level, the distance for all AUVs to travel for the horizontal survey is $w \times n$. To move to the next level, each AUV moves a distance of h. Thus, the total travel distance of AUVs is $wnL + h(L-1)n$. Therefore, the average travel distance of AUVs, S_{XS} is

$$S_{XS} = L(w+h) - h \quad (22)$$

B. The Case with an AUV failure

1) Total Survey Time: Suppose one AUV fails at an arbitrary $level\ f$. During the recovery, $n-2$ AUVs perform the survey. After the recovery node rejoins the fleet, $n-1$ AUVs perform the survey. Therefore, the entire area can be logically partitioned into three zones according to the number of AUVs performing the survey. Let $Zone\ A$, $Zone\ B$, $Zone\ C$ be the sub-areas which are surveyed by n, $n-2$, and $n-1$ AUVs respectively. Then, there are two cases to be considered for calculation of the total survey time.

- Case 1: After the recovery node rejoins the fleet of AUVs, the fleet completes the survey;
- Case 2: Before the recovery node rejoins the fleet of AUVs, other AUVs reach the end of the survey area;

In this paper, *Case 1*, the general case, will be discussed. *Case 2* can be readily extended from *Case 1*, and thus will be omitted.

Let random variable T^i represent the survey time for a d-section with i AUVs, and D_f be the time elapsed from the arrival of the fleet at a DA segment to the detection of the failure. Also, let p, q be the number of d-sections in $Zone\ A$ and $Zone\ B$ respectively. Let the total survey time for the entire area with a failure at $level\ f$ be T_f. We assume that the area of interest has exactly g number of d-sections for simplicity. Then T_f becomes

$$T_f = pT^n + qT^{n-2} + (g-p-q)T^{n-1} + D_f \quad (23)$$

Thus, the expected survey time is

$$E[T_f] = pE[T^n]+qE[T^{n-2}]+(g-p-q)E[T^{n-1}]+E[D_f] \quad (24)$$

Note that $p = min(\overline{p} : \overline{p} \times (n+K) \geq f)$ where $\overline{p} \in \mathbb{N}$. The value of q depends on when the recovery node rejoins other AUVs. For simplicity, we assume that both failure detection and reallocation of lanes occur at the same level of DA point. Then, the recovery node moves a distance of $(K+n)h$ to go back to the last sync section. Then, to cover the lane of the failed AUV up to the current DA point, it moves a distance of $(K+n)(w+h)$. Finally, it moves in a straight line for a distance of $qh(K+n-2)$ to catch up with other AUVs. Let random variable R_t be the time taken for the recovery node to move a distance of $(K+n)h + (K+n)(w+h)$ and $E[R_t]$ be the expected value of R_t. Also let R_f be the time needed for the recovery node to move a distance of $h(K+n-2)$. Then, q can be approximated as follows.

$$\begin{aligned} q &= min(\overline{q} : \overline{q} \times E[T^{n-2}] \geq E[R_t] + \overline{q}E[R_f]) \quad (25) \\ &= min\left(\overline{q} : \overline{q} \geq \frac{E[R_t]}{E[T^{n-2}] - E[R_f]}\right) \quad (26) \end{aligned}$$

Note that $E[T^n]$, $E[T^{n-1}]$, and $E[T^{n-2}]$ can be obtained using (25). The pdfs of R_t and R_f are obtained in a similar way to (13). Then, $E[R_t]$ and $E[R_f]$ are calculated based on their pdf. To approximate D_f, we simply subtract the expected survey time of the fleet in a section from the average timeout period of AUVs, i.e., $E[D_f] \approx \frac{\sum_{i=1}^{n} TO_i}{n} - E[T^n]$.

With these obtained values, the expected survey time of the fleet with a failure at $level\ f$ can be calculated from (24).

Finally, the failure can occur at any level between $level\ 1$ and $level\ L$ with a uniform probability. Then, the expected survey time with a failure at an arbitrary level, $\overline{T}_{XS}$ becomes

$$\overline{T}_{XS} = \sum_{f=1}^{L} \frac{E[T_f]}{L} \quad (27)$$

2) Average Travel Distance of AUVs: We first calculate the total distance of AUVs. Let S^i be the total travel distance of the fleet with i AUVs to survey a d-section. Then, we have

$$S^i = i \times (K+i) \times (w+h) \quad (28)$$

Let I_A, I_B, and I_C be the total travel distance of AUVs to survey $Zone\ A$, $Zone\ B$, $Zone\ C$ respectively. An AUV fails at $level\ f$ in $Zone\ A$. Therefore, I_A is

$$\begin{aligned} I_A &= np(K+n)(w+h) - (p(K+n)-f)(w+h) \quad (29) \\ &= (w+h)(p(K+n)(n-1)+f) \quad (30) \end{aligned}$$

In $Zone\ B$, the fleet performs the survey with $n-2$ AUVs. Therefore,

$$I_B = q(n-2)(K+n-2)(\frac{wn}{n-2} + h) \quad (31)$$

where q can be obtained using (26).

Similarly, the distance for the survey of $zone\ C$ is

$$I_C = (g-p-q)(n-1)(K+n-1)(\frac{wn}{n-1} + h) \quad (32)$$

Let I_R be the distance the recovery AUV moves for

the recovery and rejoining the fleet. Then, we have

$$I_R = (w+h)(K+n) + h(K+n) + qh(K+n) \quad (33)$$

$$= (K+n)(w+h(2+q)) \quad (34)$$

Then, the total travel distance of AUVs with a failure at $level\ f$, S_f is the sum of I_A, I_B, and I_C. That is,

$$S_f = I_A + I_B + I_C + I_R \quad (35)$$

The expected distance of AUVs with a failure at an arbitrary level, $\overline{S}_{XS}$, becomes

$$\overline{S}_{XS} = \frac{1}{nL}\sum_{f=1}^{L} S_f \quad (36)$$

VII. Performance Study

In this section, we present simulation results to compare the performance of XS with two other synchronization schemes, ACS and SLS.

The survey completion time and the travel distance of AUVs for surveying a rectangular area (e.g. one survey region shown in Fig. 2) have been chosen as the performance metrics. The fleet of 12 AUVs perform survey in an area of $80km^2$ ($10km \times 8km$). According to LBS, each AUV is initially responsible for a lane of $\frac{10000}{12}m \times 8000m$. The swath width of each AUV is set to $20m$, which results in $L = 400$ levels. The data transmission range of AUVs is set to be $20m$. The Discrete Gauss-Markov process model [32] is used to emulate the practical speed variation of AUVs. The initial speed and the memory level are set to $3m/s$ and 0.5 respectively (memory level of 0.0 represents a random walk mobility pattern and memory level of 1.0 results in a constant velocity fluid-flow model). Timeout periods for detection of an AUV failure are calculated with the parameters $P_o = 0.999$.

Intuitively, XS should outperform the ACS and SLS. ACS introduces a large overall synchronization overhead due to its frequent synchronization as each AUV needs to synchronize with one of its neighbors at every level. Also, an AUV in SLS has to stay at a sync line until all AUVs forward data to the Lead AUV and the AUV receives the control signal from the Lead AUV, which leads to a large sync delay, especially with a small value of K. Further, SLS requires dedicated horizontal moves of AUVs for synchronization on a sync line.

In Fig. 13 and Fig. 14, the Y axis represents the *normalized* survey time and the travel distance of AUVs, when the corresponding simulation results for ACS are set to 1. The X axis represents the ratio of K to L, denoted by u. Recall that K determines how often the AUVs in SLS or XS perform synchronization. For example, $u = 1$ (or $K = L$) means there is no synchronization during survey. Note that u does not affect the performance of ACS. Fig. 13 and Fig. 14 also show how closely the numerical estimation of the performance approximates the simulation results.

Fig. 13 compares the performance of the schemes with no AUV failure. As shown in Fig. 13(a), the survey time of XS is always lower than that of ACS or SLS due to the fact that XS introduces less synchronization. As u grows, the survey time of both XS and SLS decreases because a large value of u (or K) represents infrequent synchronization which results in less synchronization

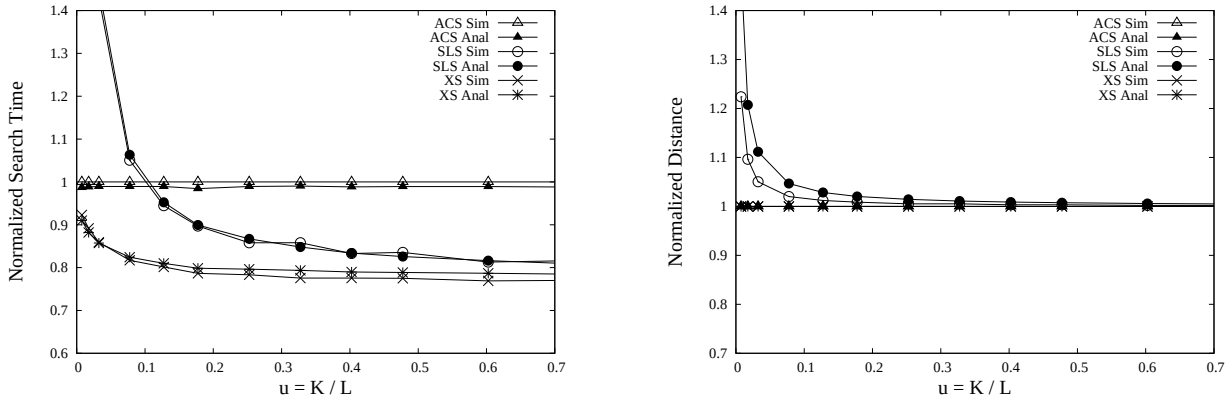

(a) Survey Time (b) Distance

Fig. 13. Varying size of K without a AUV failure

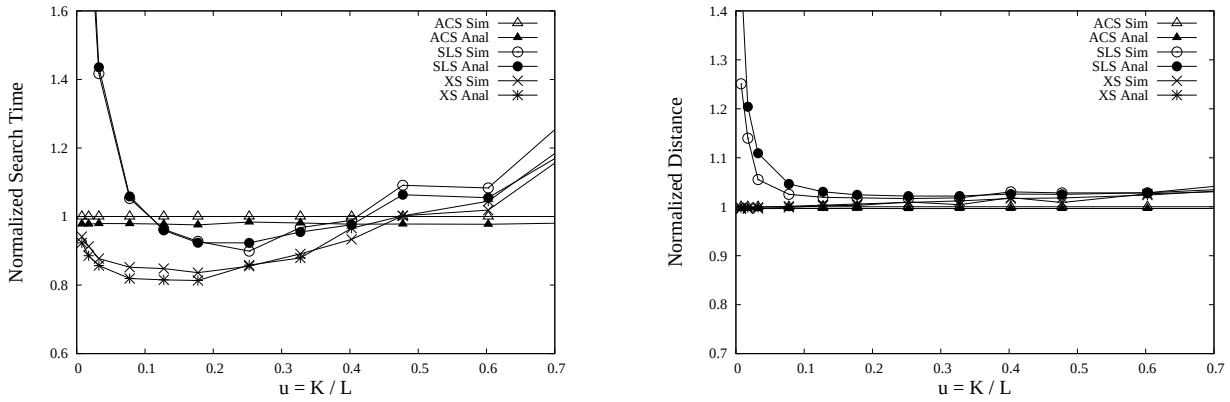

(a) Survey Time (b) Distance

Fig. 14. Varying size of K with a AUV failure

overhead, which is a positive effect on the survey time.

When there is no AUV failure, the travel distance of ACS is equal to that of XS as shown in Fig. 13(b) because the AUVs in ACS or XS follow the exactly same path determined by the LBS described in Section III. The distance of SLS is larger than that of ACS or XS due to extra movements for synchronization on sync lines. Note that XS does not require dedicated horizontal moves by AUVs for synchronization as SLS does.

Fig. 14 shows the results with an AUV failure. An AUV is set to fail at an arbitrary level. As shown in Fig. 14(a), the survey time of XS decreases as u grows until u reaches about 0.2. As u grows beyond 0.2, however, the survey time of XS increases, and eventually becomes larger than that of ACS. This comes from the fact that a large value of u (or K) has negative effects on the survey time unlike in the case of no AUV failure. Suppose that an AUV fails at an arbitrary position. A large value of K causes a large amount of time for the recovery node to go back to the last RP and survey. Thus, the fleet has to survey with only $(n-2)$ AUVs for a long time until the recovery node rejoins. Further, it is possible that other

AUVs arrive at the end of the survey area before the recovery AUV rejoins. In this case, the survey will not be completed until the recovery AUV arrives at the end of the survey area. Due to both the negative and positive effects of K, there is an optimal value of K which results in the minimum survey time.

As shown in Fig. 14(b), SLS has the largest average distance. XS and ACS have almost same travel distance when the value of u is small. Note that the travel distance of XS increases as u grows. The difference between the travel distances of XS and ACS, however, is less than 5% of the travel distance of ACS even in the case of a large value of u.

VIII. Concluding Remarks

The work represents the first attempt to the design and qualitative as well as quantitative analysis of search and survey algorithms using cooperative AUVs with failure tolerance.

In this paper, we have proposed a rendezvous algorithm, X Synchronization, for cooperative search and survey using a fleet of AUVs with limited energy and communication capabilities. XS enables AUVs to survey a large area for time-sensitive applications tolerating AUV failures via mobility-assisted data communication. We have derived appropriate synchronization timeout periods to reduce the number of false alarms by estimating the arrival time of AUVs. A numerical model has also been devised to approximate the survey time and traveling distance of AUVs. Results from simulations and numerical analysis show that XS can outperform two other rendezvous algorithms (ACS and SLS) in terms of the total survey time and the travel distance of AUVs.

IX. Acknowledgement

The authors would like to thank Bill Collins of Quester Tangent Corp. for his useful suggestions.

References

[1] B. Jalving, G. K., H. O. K., and V. K., "A toolbox of aiding techniques for the HUGIN AUV integrated inertial navigation system," in *Oceans*, Piscataway, NJ, 2003.

[2] J. Heidemann, W. Ye, J. Wills, A. Syed, and Y. Li, "Research challenges and applications for underwater sensor networking," in *Proceedings of the IEEE Wireless Communications and Networking Conference*. Las Vegas, Nevada, USA: IEEE, April 2006, pp. 228–235.

[3] T. M. Ian F. Akyildiz, D. Pompili, "Underwater acoustic sensor networks: Research challenges," *Ad Hoc Networks (Elsevier)*, vol. 3, pp. 257–279, 2005.

[4] E. Sozer, M. Stojanovic, and J. Proakis, "Underwater acoustic networks," *IEEE Journal of Oceanic Engineering*, vol. 25, no. 1, pp. 72–83, 2000.

[5] J. W. Bales and C. Chryssostomidis, "High bandwidth, low-power,short-range optical communication underwater," in *Proceedings of 9th Internationa Symposium on Unmanned Untethered Submersible Technology*, 1995.

[6] J. Delaney, A. Chave, G. R. Heath, B. Howe, and P. Beauchamp, "Neptune: real-time, long-term ocean and earth studies at the scale of a tectonic plate," in *OCEANS, MTS/IEEE Conference and Exhibition*, vol. 3, Honolulu, HI, USA, 2001, pp. 1366–1373.

[7] R. A. Stephen, "Ocean seismic network seafloor observatories," *Oceanus*, pp. 33–37, March 1998.

[8] M. Grasmueck, G. P. Eberli, D. A. Viggiano, T. Correa, G. Rathwell, and J. Luo, "Autonomous underwater vehicle (AUV) mapping reveals coral mound distribution, morphology, and oceanography in deep water of the straits of florida," *GEOPHYSICAL RESEARCH LETTERS*, vol. 33, 2006.

[9] D. R. Yoerger, M.Jakuba, A. M. Bradley, and B. Bingham, "Techniques for deep sea near bottom survey using an autonomous underwater vehicle," *International Journal of Robotics Research archive*, vol. 26, pp. 41,54, October 2007.

[10] D. Fornari, M. Tivey, H. Schouten, M. Perfit, K. V. Damm, D. Yoerger, A. Bradley, M. Edwards, R. Haymon, T. Shank, D. Scheirer, and P.Johnson, "Submarine lava flow emplacement processes at the east pacific rise 9 50'n: Implications for hydrothermal fluid circulation in the upper ocean crust," *The Thermal Structure of the Ocean Crust and Dynamics of Hydrothermal Circulation*, vol. 148, 2004.

[11] M.-H. Cormier, W. B. Ryan, A. M. Bradley, D. R. Yoerger, A. Shah, J. Sinton, R. Batiza, and K. Rubin, "Variable extrusive emplacement mechanisms in the axial region of the east pacific rise," *Geology*, vol. 31, no. 7, 2003.

[12] E. Fiorelli, N. Leonard, P. Bhatta, D. Paley, R. Bachmayer, and D. Fratantoni, "Multi-AUV control and adaptive sampling in Monterey bay," in *Proceedings of IEEE Autonomous Underwater Vehicles: Workshop on Multiple AUV Operations (AUV04)*, June 2004.

[13] J. Catipovic, D. Brady, and S. Etchemendy, "Development of underwater acoustic modems and networks," *Oceanography*, vol. 6, pp. 112–119, 1993.

[14] M. Stojanovic, "Recent advances in high-speed underwater acoustic communications," *IEEE Journal of Oceanic Engineering*, vol. 21, pp. 125–136, 1996.

[15] L. Freitag, M. Stojanovic, M. Grund, and S. Singh, "Acoustic communications for regional undersea observatories," in *Oceanology International*, London, U.K, 2002.

[16] N. Farr, A. Chave, L. Freitag, J. Preisig, S. White, D. Yoerger, and F. Sonnichsen, "Optical modem technology for seafloor observatories," in *Proceedings of IEEE OCEANS*, September 2006, pp. 1–6.

[17] J. Joe and S. H. Toh, "Digital underwater communication using electric current method," *OCEANS 2007*, pp. 1–4, 2007.

[18] G. Wang, G. Cao, and T. L. Porta, "Movement-assisted sensor deployment," in *IEEE INFOCOM Conference Proceedings*, March 2004.

[19] J. Wu and S. Yang, "Smart: A scan-based movement-assisted sensor deployment method in wireless sensor networks," in *IEEE INFOCOM Conference Proceedings*, March 2005.

[20] B. Liu, P. B. O. Dousse, P. Nain, and D. Towsley, "Mobility improves coverage of sensor networks," in *ACM MobiHoc*, 2005.

[21] A. Khan, C. Qiao, and S. K. Tripathi, "A failure-tolerant mobile traversal scheme based on triangulation coverage," in *Proceedings of International Conference on Heterogeneous Networking for Quality, Reliability, Security and Robustness (Qshine) and ICC 2007*, Vancouver, Canada, August 2007.

[22] (2005, August) Abe: The autonomous benthic explorer. [Online]. Available: http://www.whoi.edu/sbl/liteSite.do? litesiteid=4050&articleId=6343

[23] (2005, October) Unmanned aircraft systems roadmap 2005-2030. [Online]. Available: http://www.fas.org/irp/program/collect/ uav_roadmap2005.pdf

[24] R. Behringer, W. Travis, R. Daily, D. Bevly, W. Kubinger, and W. H. V. Fehlberg, "Rascal - an autonomous ground vehicle for desert driving in the darpa grand challenge 2005," in *Poceedings of IEEE Intelligent Transportation Systems*, September 2005, pp. 644–649.

[25] C. W. Reynolds, "Flocks, herds, and schools: a distributed behavioral model," *Computer Graphics*, vol. 21, no. 6, pp. 25–34, July 1987.

[26] T. Vicsek, A. Czirok, E. B. Jacob, I. Cohen, and O. Schochet, "Novel type of phase transitions in a system of self-driven particles," *Physical Review Letters*, vol. 75, pp. 1226 – 1229, 1995.

[27] A. Jadbabaie, J. Lin, and A. S. Morse, "Coordination of groups of mobile autonomous agents using nearest neighbor rules," *IEEE Transactions on Automatic Control*, vol. 48, pp. 988 – 1001, June 2003.

[28] X. Cui, T. Hardin, R. K. Ragade, , and A. S. Elmaghraby, "A swarm-based fuzzy logic control mobile sensor network for hazardous contaminants localization," in *The IEEE International Conference on Mobile Ad-hoc and Sensor Systems (MASS 2004)*, FortLauderdale, Florida, U.S.

[29] D. Payton, M. Daily, R. Estowski, M. Howard, and C. Lee, "Pheromone robotics," *Autonomous Robots*, vol. 11, no. 3, pp.

319–324, November 2001.

[30] P. E. Rybski, S. Stoeter, M. D. Erickson, M. L. Gini, D. F. Hougen, and N. Papanikolopoulos, “A team of robotic agents for surveillance,” in *Fourth International Conference on Autonomous Agents (Agents 2000)*.

[31] Image of mid-atlantic ridge. [Online]. Available: http://www.ngdc.noaa.gov/

[32] B. Liang and Z. J. Haas, “Predictive distance-based mobility management for multidimensional pcs networks,” *IEEE/ACM Transcations on Networking*, vol. 11, no. 5, pp. 718 – 732, October 2003.